ESD-TR-83-075
Reprinted from PROCEEDINGS OF THE SIXTEENTH IEEE
PHOTOVOLTAIC SPECIALISTS CONFERENCE, September 1982

OPTIMAL DESIGN OF HIGH-EFFICIENCY TANDEM CELLS

John C. C. Fan, B-Y. Tsaur, and B. J. Palm

Lincoln Laboratory, Massachusetts Institute of Technology
Lexington, Massachusetts 02173

ABSTRACT

Computer analysis indicates that a substantial increase in solar cell conversion efficiencies can be achieved by using two-cell, multi-bandgap tandem structures instead of single-junction cells. Practical AM1 efficiencies of about 30% at one sun and over 30% at multiple suns are to be expected. The further increases in efficiency calculated for a three-cell tandem structure are much smaller and may not justify the added complexity. For inexpensive two-cell tandem modules, Si is preferred for the bottom cell, and the top-cell material should have a bandgap of 1.75 to 1.80 eV. The GaAs-AlAs and GaAs-GaP systems are very attractive candidates for the top cell. Significant advances have been achieved in growing GaAs on Ge-coated Si substrates (for the two-terminal, two-cell structure) and in growing free-standing ultrathin GaAs layers (for the two-terminal or four-terminal structures). These advances should be transferable to the GaAs-AlAs and GaAs-GaP systems.

INTRODUCTION

Before solar photovoltaic conversion can provide a significant portion of the energy needs of the U.S. and the world, photovoltaic systems must satisfy two major requirements: the system costs must be competitive with other means of energy generation and the amount of energy generated during the life cycle of a system must be substantially greater than the energy required to fabricate the system. In other words, the conversion systems must be both inexpensive and efficient.

According to calculations by various workers (1,2), the allowable cost per unit area of solar cell modules depends strongly on module efficiency. This dependence results from the large area-related balance-of-system (ARBOS) costs. Included in ARBOS costs are site preparation, structural supports, electric wiring, and installation labor. Assuming the U.S. Department of Energy 1986 goal of ARBOS cost of $60/m^2$, a module price of $0.7 per peak watt and module efficiency of 14% at AM1, Bowler and Wolf (1) have calculated curves relating the tradeoff between cell cost and module efficiency for flat-plate modules (see Fig. 1). For example, a

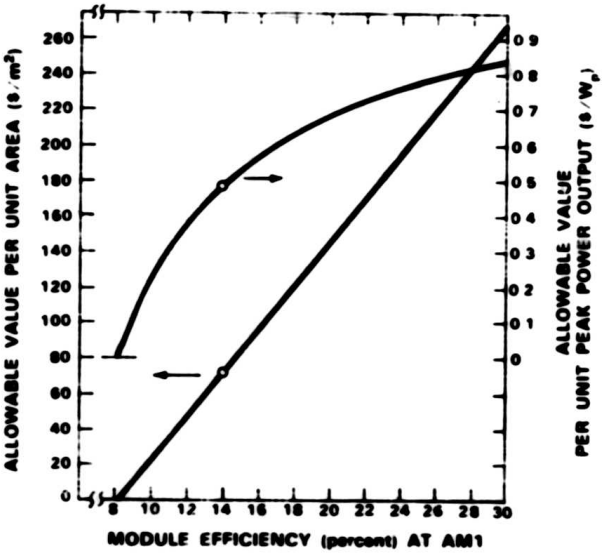

Fig. 1. Relationship between the allowable value of solar cells in dollars per square meter or dollars per peak watt and the cell module efficiency.

20% cell costing 7 times as much as a 10% cell of the same area will yield equivalent overall photovoltaic system costs. For a 30% cell, the cost can be about 14 times the cost of the 10% cell. Therefore, if the cost of fabricating high-efficiency cells is low enough, such cells will have a substantial economic advantage over low-efficiency cells. The advantage will be even greater if the area-related costs incurred during solar cell fabrication, for example, the costs of antireflection coatings and contact fingers, are included in the calculation. In addition, the use of concentrating systems can further enhance the cost advantage of high-efficiency cells. If balance-of-system costs remain high, high-efficiency cells may well be the only cells that would be economical for large-scale terrestrial applications. For space applications, high-efficiency cells also have significant payload advantages. This paper will concentrate on the design of high-efficiency, flat-plate, multi-bandgap cells, although many of the results are also applicable for concentrator cells.

SINGLE-JUNCTION CELLS

Before we consider multi-bandgap cells, we shall examine the conversion efficiencies of single-bandgap cells. For such cells, Fig. 2 shows

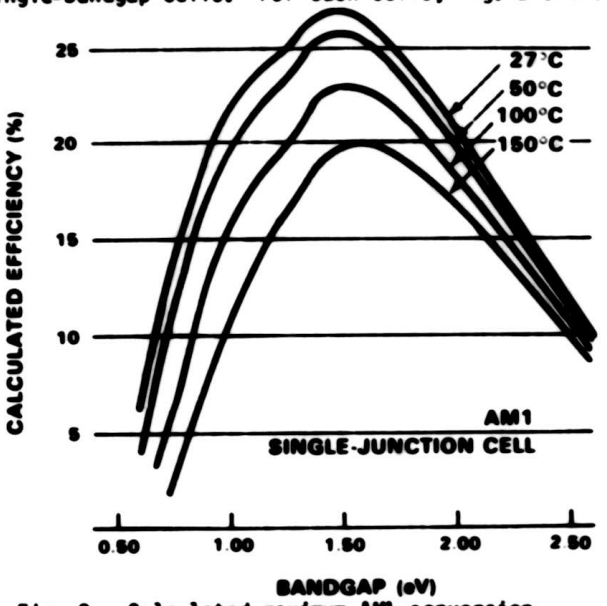

Fig. 2. Calculated maximum AM1 conversion efficiencies at 27, 50, 100 and 150°C of single-junction solar cells made of materials having various bandgap energies.

the theoretical maximum conversion efficiencies at AM1 calculated as a function of energy gap for various operating temperatures. (The formulation of the calculations is given in the Appendix.) The results should be applicable to all kinds of junctions, including p-n, Schottky, and heterojunctions. In the case of heterojunctions, the maximum calculated efficiency depends primarily on the energy gap of the semiconductor that absorbs the bulk of solar photons.

For single-junction cells, as shown in Fig. 2, the highest theoretical AM1 efficiencies are for energy gaps between 1.45 and 1.5 eV, for which values of about 27.5% at an operating temperature of 27°C can be expected. Efficiencies of 21-22% at AM1 have been reported (3,4) for gallium arsenide (GaAs), which has a bandgap (E_g) about 1.43 eV. For silicon (Si) -- E_g = 1.1 eV -- the calculated conversion efficiency at 27°C is about 23% at AM1, and Si cells have achieved an efficiency of 18% (5). The conversion efficiencies will decrease with increasing operating temperature, especially for lower bandgap materials such as Si. Although small incremental increases in efficiency can still be expected as refinements are made to existing cell designs, a different strategy must be used to obtain much higher efficiencies.

MULTI-BANDGAP CELLS

The utilization of multi-bandgap cells could greatly boost conversion efficiency. The principles of this approach were suggested in 1955 (6). A single-junction cell can convert only a fraction of the incident sunlight into electricity. Such a cell can be designed to be optimally efficient in a limited energy range. Dividing the solar spectrum into such energy ranges and making each range incident upon an appropriately designed cell would result in great improvements in overall conversion efficiency.

In one configuration, solar cells with different energy gaps are stacked in tandem so that the cell facing the sun has the largest energy gap (see Fig. 3). This top cell absorbs all the

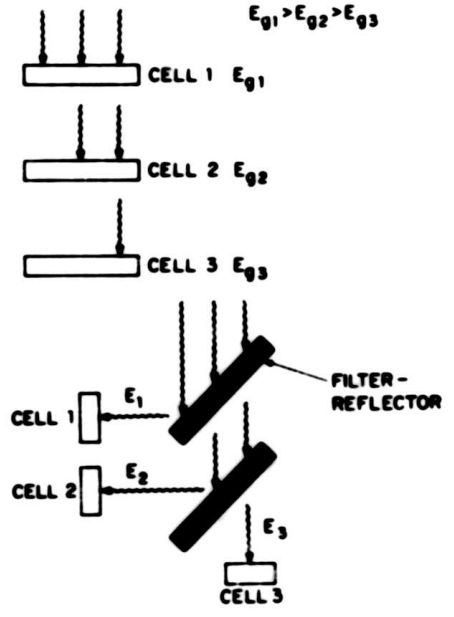

Fig. 3. Spectrum-splitting schemes for achieving high conversion efficiencies. Above, tandem cells; below, filter-reflectors.

transmitted photons at and above its energy gap and transmits the less energetic photons to the cells below. The next cell in the stack absorbs all the transmitted photons with energies equal to or greater than its energy gap, and transmits the rest downward in the stack, etc. In principle, any number of cells can be used in tandem.

Designing tandem cells is more complex than designing a single-junction cell. For example, each cell must transmit efficiently the photons with less than its bandgap energy. The contacts on the backs of the upper cells must be transparent to these photons and, therefore, cannot be made of the usual bulk metal layers. If the cells in a stack are connected separately, different external load circuits must be provided for each cell. However, if the cells are connected in series, the thicknesses and bandgaps of individual cells in the stack must be adjusted so that the photocurrents in all the cells are equal. Despite these difficulties, there is a potential for large increases in conversion efficiency from tandem cells.

Optical filter-reflector systems can be designed to split the solar spectrum into several different energy ranges and to direct each range upon cells that are designed for optimum conversion in that range (see Fig. 3). Unlike stacked tandem cells, the cells in filter-reflector systems need not be arranged in order of decreasing energy. However, individual external circuit loads are necessary for each constituent cell. Also, optical systems are usually less than 100% efficient, so that some light energy is lost in the filtering and reflection processes. Such loss is detrimental to performance and can cause heating problems in the optics as absorbed light is converted to thermal energy. This configuration is also difficult to use for high-efficiency flat-plate modules.

Maximum theoretical efficiencies can be calculated for multi-bandgap cells. Previously, studies were made (7-9) for such cells under high solar concentration. Since there has been increasing interest in designing high-efficiency flat-plate modules, most of our calculations will be based on flat-plate, non-concentrating designs. To a large extent, however, the results should also apply to concentrating systems as well as to filter-reflector systems.

A two-cell tandem system is the simplest case. Figure 4 shows the various configurations of such a

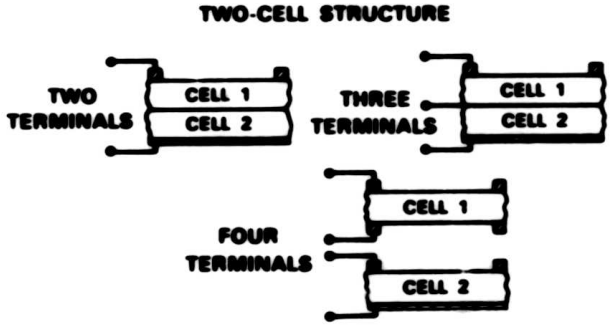

Fig. 4. Schematic diagrams of various electrical connections to a two-cell tandem system. The two cells can be connected to form either two-, three- or four-terminal devices.

system. The two cells can be connected to form either two-terminal, three-terminal or four-terminal devices. In a two-terminal device, the cells are connected in series; as stated above, the photocurrents in the two cells must be equal for optimal operation. In contrast, in the three- and four-terminal cells the photocurrents do not have to be equal. As shown in Fig. 5, it is straightforward to connect two- or four-terminal devices in series for high voltage operation. However, it is very difficult to connect three-terminal devices in series. Figure 5 shows one of several complicated connections possible for these devices (10). Each of the three-terminal devices is connected to a second cell, which must have a photocurrent close to that of the bottom cell of the three-terminal structure and a

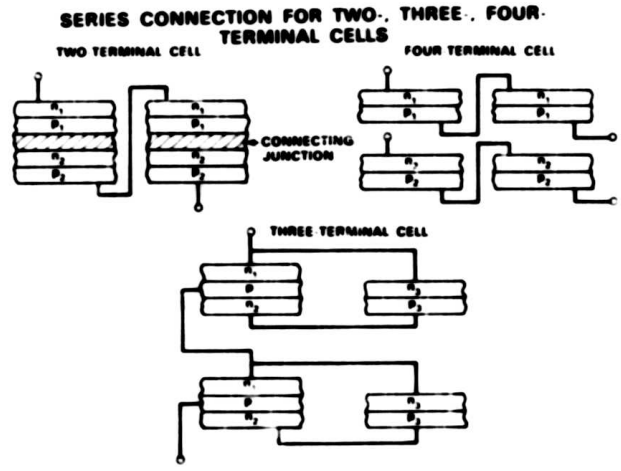

Fig. 5. Series connections for two-, three-, and four-terminal tandem cells for high-voltage operation.

photovoltage equal to the difference in photovoltage between the bottom cell and the top cell. Because of this severe limitation, three-terminal tandem cells do not appear to be very viable, and they will not be discussed further.

To compare the relative merits of two- and four-terminal tandem cells, one must understand the essential difference betweeen these devices. In a two-terminal structure, only one external circuit load is needed, but the requirement of photocurrent matching greatly limits the choice of energy gaps of the two cells. Figure 6 shows the dependence of

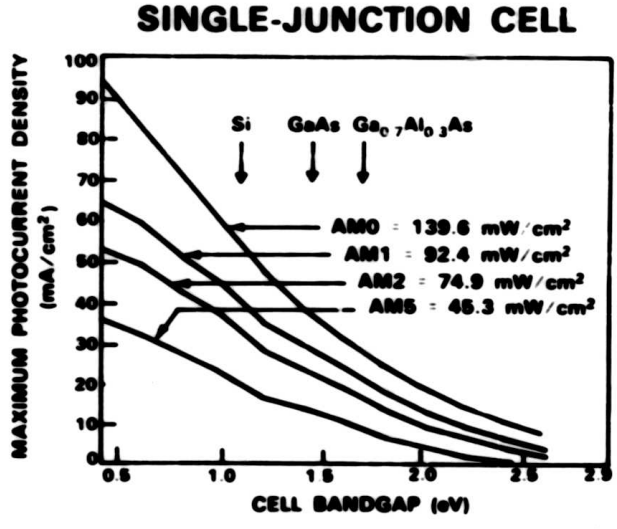

Fig. 6. Calculated maximum AM0, AM1, AM2 and AM5 photocurrent densities of solar cells as a function of the energy gaps of the cell materials.

the calculated maximum photocurrent densities on energy gap for different air masses. Since the spectral distributions (11) of various air masses are different, this dependence is not the same for different air masses. Therefore, an optimal design of a two-terminal tandem cell for all air masses is

not simple. In the four-terminal case, two separate external circuit loads are used. Since the two individual cells are not coupled, the photocurrents do not have to be the same. Consequently, a much larger selection of combinations of energy gaps is possible, and effects of spectral variations on photocurrents do not pose serious limits. These tradeoffs have been calculated, in order to ascertain the optimal selections. The calculations are based on the model given in the Appendix.

Figures 7 and 8 are AM0 and AM1 iso-efficiency plots for the two-cell, two-terminal tandem

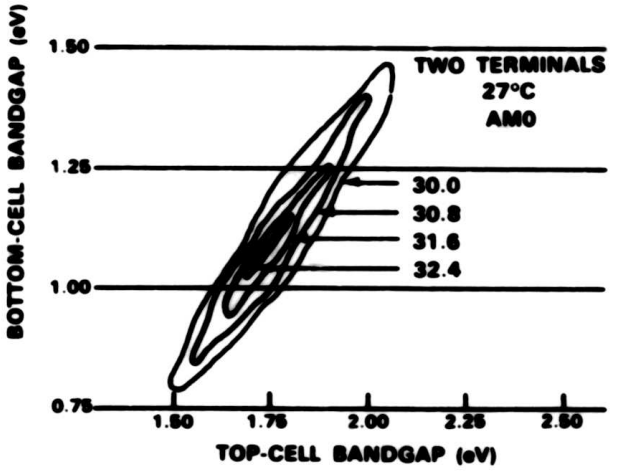

Fig. 7. AM0 iso-efficiency plots for the two-cell, two-terminal tandem structure at 27°C and one sun.

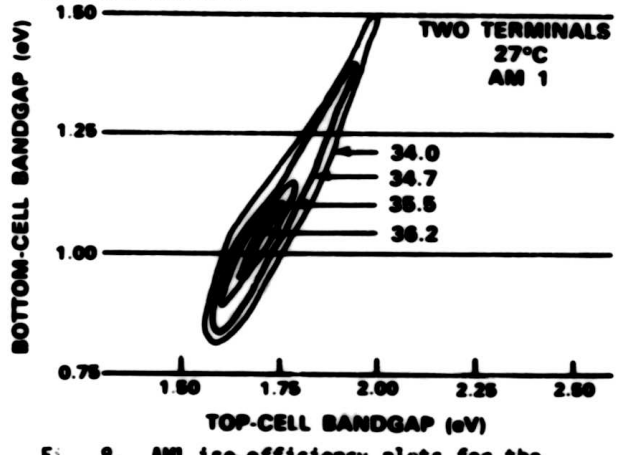

Fig. 8. AM1 iso-efficiency plots for the two-cell, two-terminal tandem structure at 27°C and one sun.

structure at 27°C and one sun. The maximum theoretical efficiencies for this system are 32.4% at AM0 and 36.2% at AM1. Although practical efficiencies should be about 5-6% lower, these values are still considerably higher than the value of 22% at AM1 obtained for the best single-junction cells. For the two-terminal structure, for optimal efficiencies the allowable range of energy gaps for the top and bottom cells is very narrow. For both AM0 and AM1, the top cell should have an energy gap of about 1.75 eV, and the bottom cell about 1.1 eV. This combination is very fortunate, since it allows the use of Si (E_g = 1.1 eV) for the bottom cell, a great advantage for the realization of inexpensive tandem cells.

Using these optimal energy gap values, we have calculated the photocurrents generated in each cell

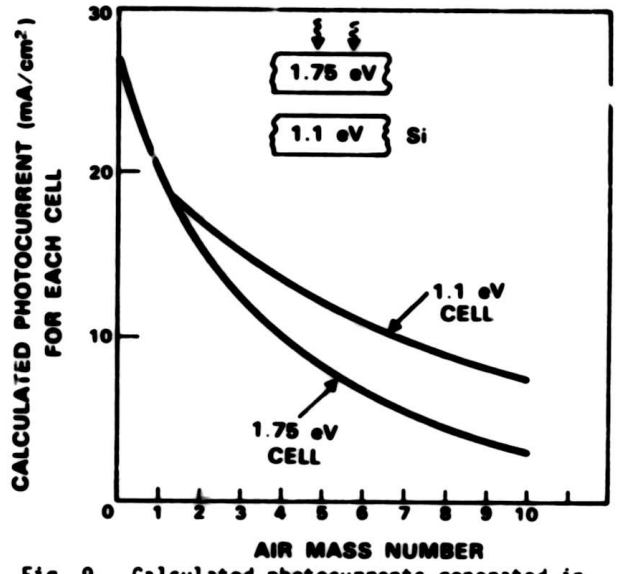

Fig. 9. Calculated photocurrents generated in cells with bandgaps of 1.75 eV and 1.1 eV as a function of air mass.

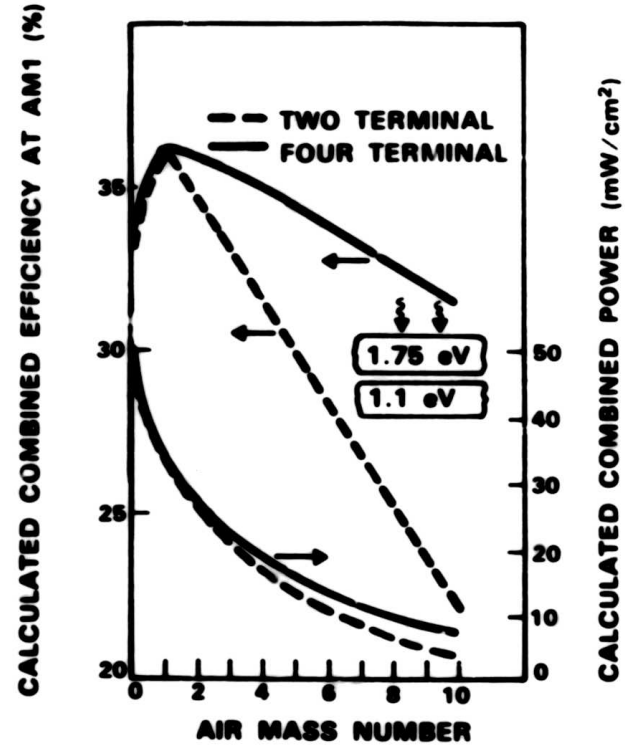

Fig. 10. Calculated combined AM1 efficiency and output power of two- and four-terminal two-cell tandem structures as a function of air mass.

at different air masses. Between AM0 and AM1.5, the two photocurrents remain the same. However, with increasing air mass the photocurrent in the bottom cell increases with respect to the top cell (see Fig. 9), since the solar spectral distributions shift toward lower photon energies. At AM10, the photocurrent is about a factor of two larger for the bottom cell than for the top cell. Since the smaller photocurrent dominates in a series-connected two-terminal structure, the conversion efficiency sharply decreases, as shown in Figure 10.

Because photocurrent matching is not necessary for a four-terminal tandem structure, a much smaller decrease in conversion efficiency occurs with increasing air mass (as shown in Fig. 10). Although there is a large difference in conversion efficiency between the two- and four-terminal structures, the net difference in output electrical power is reduced because of the much smaller sunlight intensity at the higher air masses. Therefore, the net power loss for a two-terminal structure is not too severe (see Fig. 10).

Nevertheless, the four-terminal structure has an important advantage over the two-terminal structure. Because the two photocurrents do not have to match, a wide range of bandgap energies is allowable for the top and bottom cells. Figures 11

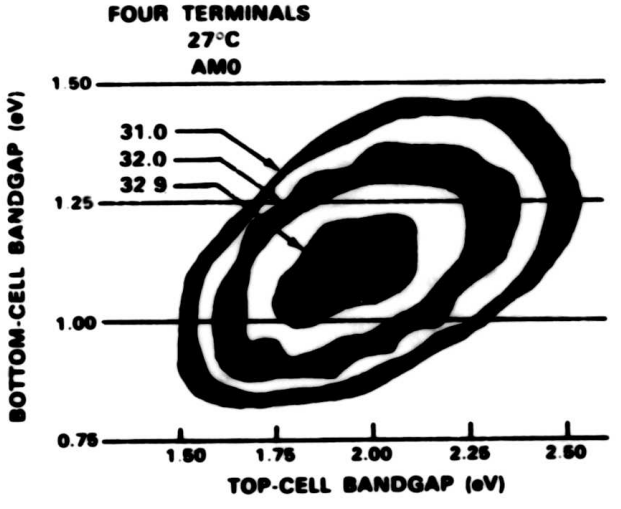

Fig. 11. AM0 iso-efficiency plots for the two-cell, four-terminal tandem structure at 27°C and one sun.

and 12 show the AM0 and AM1 iso-efficiency curves at 27°C for tandem structures where the two cells are separately connected. The maximum calculated efficiencies for this system are 32.9% at AM0 and 36.6% at AM1, slightly higher than those of the two-terminal structure. Practical efficiencies are expected to be about 5-6% lower. It is interesting to note that a realistic efficiency of about 30% at AM1 can be achieved for a flat-plate non-concentrating tandem device with just a

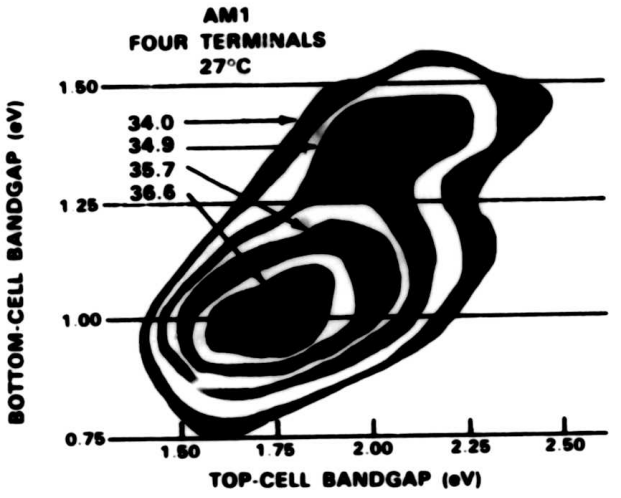

Fig. 12. AM1 iso-efficiency plots for the two-cell, four-terminal tandem structure at 27°C and one sun.

two-cell structure. There is a wide selection of acceptable energy gaps. If for economic reasons Si is used for the bottom cell, then the top cell should be about 1.8 eV for either AM0 or AM1. This combination of 1.1 eV and 1.8 eV is very close to the optimal selection of 1.1 eV and 1.75 eV for the two-terminal tandem structure.

In the four-terminal case, maximum efficiency can be achieved at 27°C for bottom-cell materials with lower bandgaps than Si. However, these materials are less suitable for operation at higher temperatures. This effect is illustrated by Fig. 13, where the AM1 conversion efficiencies

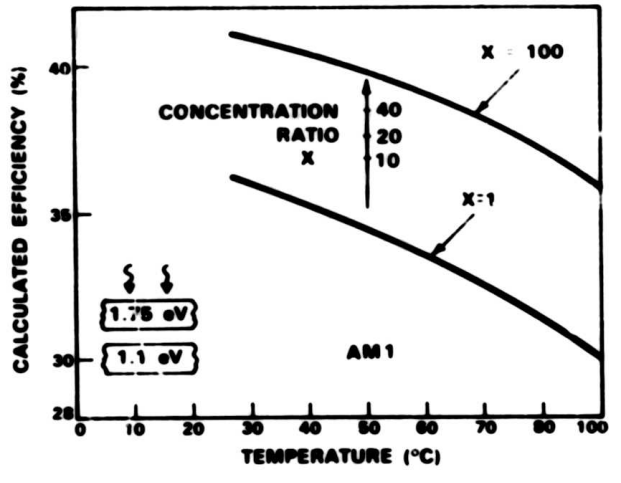

Fig. 13. Calculated AM1 conversion efficiency of a tandem structure (with a 1.75 eV top cell and 1.1 eV bottom cell) as a function of operating temperature at one sun and one hundred suns.

calculated for a two-cell tandem structure (E_{g1} = 1.75 eV and E_{g2} = 1.1 eV) at concentration ratios of 1 and 100 are plotted as a function of

operating temperature. (The results are the same for either two- or four-terminal cells.) With increasing temperature, the dark saturation currents of the two cells increase, causing the photovoltages to decrease. At 50°C, which is a common operating temperature for flat-plate modules, the efficiency at one sun has decreased from 36.2% to 34.3%. At 100°C, the efficiency drops to 29.8%. The decrease in efficiency could be reduced by using a bottom cell material with an even higher bandgap than Si, since the dark saturation current decreases with increasing bandgap. However, there is a compelling economic reason to use Si for the bottom cell, and the decrease in photovoltage can be largely compensated by a modest amount of concentration, as shown in Fig. 13. For a concentration ratio of only 10, the efficiency at 50°C increases from 34.2% to 36.9%. Larger concentration ratios increase the efficiencies further, but at a slower rate. In fact, on the basis of our model, the conversion efficiencies increase logarithmically with the concentration ratios. Therefore, substantial beneficial effects can be obtained with only small concentration ratios, which are easily attainable.

We have shown that there are significant gains in efficiency in going from a single-junction cell to a two-cell tandem structure. However, the gains in conversion efficiency from a two-cell to a three-cell tandem structure are disappointing. Figures 14 and 15 show the AM1 iso-efficiency plots

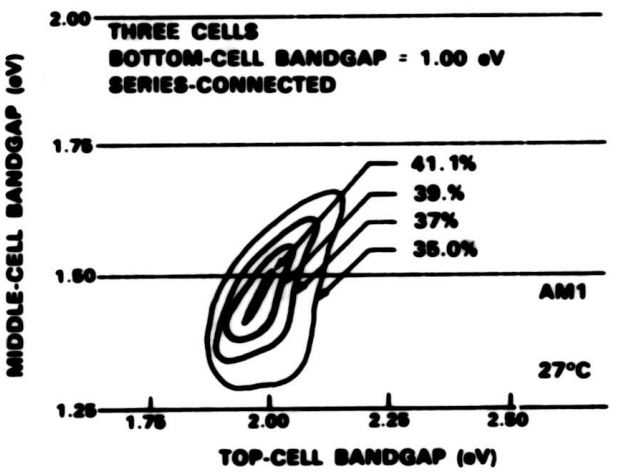

Fig. 14. AM1 iso-efficiency plots for the three-cell tandem structure where the cells are series connected. The bottom cell has a fixed energy gap of 1.0 eV. The structure is at 27°C and one sun.

at 27°C for the three-cell tandem structure with the cells connected in series and separately, respectively. The curves are plotted for a bottom-cell energy gap of 1.0 eV. (The maximum calculated efficiencies for the three-cell structure are obtained when this energy gap is 0.95-1.0 eV). The maximum theoretical efficiency at AM1 is 41.1% for the series-connected structure and 42.5% for the separately connected structure,

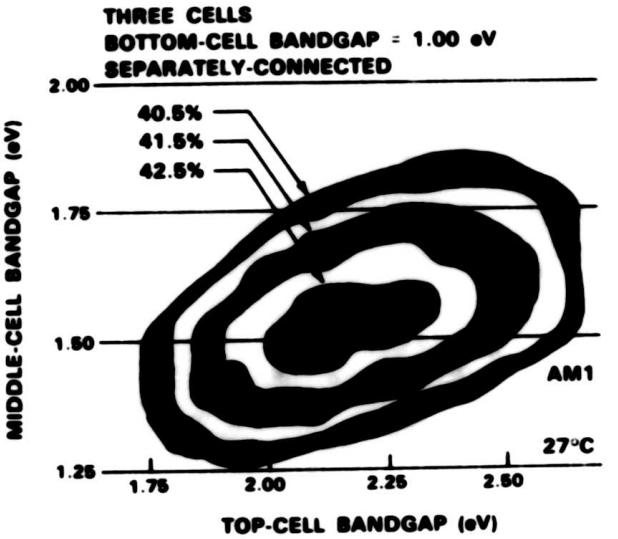

Fig. 15. AM1 iso-efficiency plots for the three-cell tandem structure where the cells are separately connected. The bottom cell has a fixed energy gap of 1.0 eV. The structure is at 27°C and 1 sun.

and these values are only about 5-6% higher than those of two-cell tandem structures. These modest increases in efficiency may not justify the substantial increase in complexity that would be necessary for the fabrication of three-cell structures. In addition, if Si is selected for the bottom cell the theoretical conversion efficiencies are further limited. With Si for the bottom cell, the only combination allowed for series-connected structures is 2.05 eV for the top cell and 1.55 eV for the middle cell, giving a conversion efficiency of only 40.0% at AM1. For separately connected structures, quite a few combinations of bandgap energies are allowed (for example, 2.15 eV for the top cell, 1.60 eV for the middle cell). The maximum theoretical AM1 efficiency is 41.4%, which is less than 5% higher than that calculated for a two-cell Si-based tandem structure. Therefore, except for space applications where the incremental increases in conversion efficiencies may be justified, three-cell tandem structures are not very cost effective and will not be discussed further in this paper.

TWO-CELL TANDEM STRUCTURES

It was shown above that for two-cell structures the optimum combination of energy gaps is 1.0-1.1 eV for the bottom cell and 1.75-1.80 eV for the top cell. Reference 10 shows that quite a number of semiconductors fall in each range (see Fig. 16). However, for economic reasons, Si is the best choice for the bottom cell. The top cell could be fabricated from $Ga_{1-x}Al_xAs$ or $Ga_{1-x}P_xA_s$ with x about 0.3. Amorphous silicon-hydrogen alloys (a-Si:H) could also be used. The energy gaps of these alloys can vary from about 1.6 to 2.0 eV, depending on the hydrogen content (12). Therefore, a tandem structure composed of an a-Si:H cell on

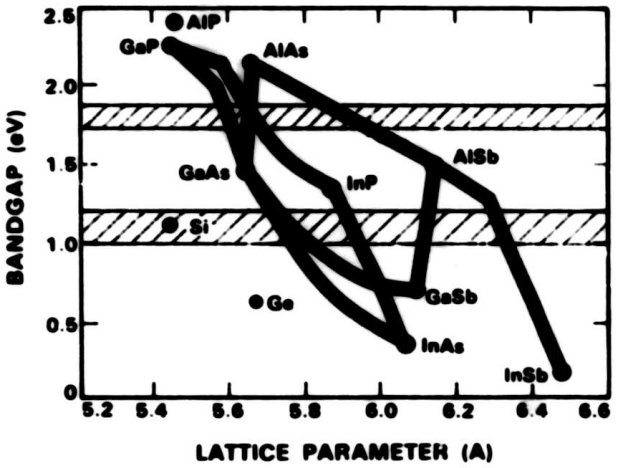

Fig. 16. Bandgap energies and lattice constants for III-V and elemental semiconductors.

top of a crystalline Si cell appears to be very attractive, especially because there are no lattice matching problems, a major concern in crystalline monolithic structures. However, the a-Si:H cell must be very efficient, since it is not advantageous to have a low-efficiency cell on the top of the stack. The top cell, which has the higher photovoltage, makes a much larger contribution to the combined efficiency. For example, for a two-cell structure with 1.75 eV and 1.1 eV, the calculated combined AM1 efficiency of 36.2% is composed of 24.9% from the top cell and 11.3% from the bottom cell.

There are a number of other semiconductors that have energy gaps in the range of 1.7-1.8 eV, including CdSe, $ZnGeP_2$, and $AgGaSe_2$ (13). However, these materials are less developed than the III-V compounds, and their potential applications are further in the future. If a two-terminal structure is to be grown monolithically, lattice matching between the two cells is very critical. Figure 16 shows the energy gaps of a number of semiconductors as a function of their lattice constants. The lattice constant of Si is about 4% lower than those of the GaAs-AlAs alloys. The GaAs-GaP system can also provide materials with energy gaps in the vicinity of 1.75 eV. These materials will have a smaller lattice mismatch with Si. However, the growth temperatures are normally higher for GaAs-GaP than for GaAs-AlAs, potentially causing more severe thermal cracking problems. Both GaAs-AlAs and GaAs-GaP alloys have thermal expansion coefficients much smaller than that of Si.

EXPERIMENTS ON TANDEM CELLS

With the objective of developing high-efficiency tandem cells, we have been investigating the growth of GaAs layers on Si substrates by chemical vapor deposition (CVD). If this work is successful, the technology should be transferable to the GaAs-GaP and GaAs-AlAs systems. The large lattice mismatch between GaAs and Si produces severe misfit dislocations at the interface between the two materials. We have been working on techniques to minimize the density of misfit dislocations threading out of the interface into the GaAs layer. Partial success has already been attained. Figure 17 is a schematic diagram of

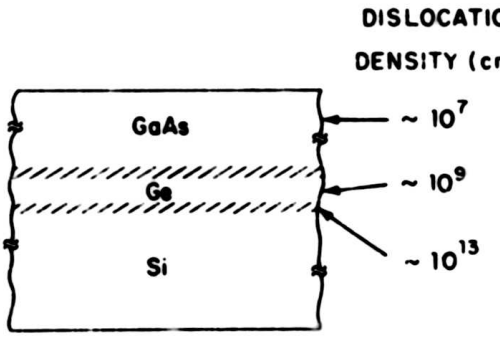

Fig. 17. Schematic of GaAs/Ge/Si cross section summarizing the dislocation densities measured by transmission electron microscopy.

a GaAs solar cell deposited on a Ge-coated Si substrate, showing the dislocation densities measured by transmission electron microscopy. By using a Ge interface layer, the dislocation density in the GaAs layer is lowered to 10^7 cm^{-2}, and solar cells with efficiency of about 12% at AM1 have been obtained (14). Very recently, by using thermal cycling procedures during GaAs growth, we have further lowered the dislocation densities (15), and conversion efficiencies of small-area cells have increased to about 14%.

The structure shown in Fig. 17 has a heavily doped p^+ Si substrate. When we used a low-doped p Si substrate, an n-p junction was formed in the Si by diffusion of As during GaAs growth. We have obtained (15) tandem effects with an open-circuit voltage $V_{oc} \sim 1.2$ eV and a short-circuit current density $J_{sc} \sim 7$ mA/cm^2 without any antireflection coating. The important result of these experiments is that the Ge layer serves not only as a barrier against the propagation of misfit dislocations but also as a low-resistance interconnect between the GaAs and Si cells. We believe that the defects in the Ge layer produce high leakage currents between the heterojunctions formed at the GaAs-Ge and Ge-Si interfaces, so that no tunnel junction is needed.

The photocurrents generated in the GaAs and Si cells in the monolithic structure are not the same. At AM1, Si can only generate about 11 mA/cm^2 after the solar spectrum is filtered by GaAs. Therefore the maximum theoretical combined efficiency of the monolithic structure is only about 15% at AM1. However, we propose a novel design that would greatly increase the photocurrent. The key idea is to etch away part of the GaAs cell, exposing the Si cell underneath. The photocurrent in the Si cell will disproportionately increase, and the combined efficiency will greatly increase. We have

calculated that if 32% of the area of the GaAs cell is removed, the photocurrents generated in the GaAs and Si cells will be equal, and the theoretical combined efficiency will be increased to nearly 30% at AM1.

For two-terminal monolithic tandem structures composed of a bottom Si cell (E_g = 1.1 eV) and top cell with energy gap E_{g1}, Fig. 18 shows the

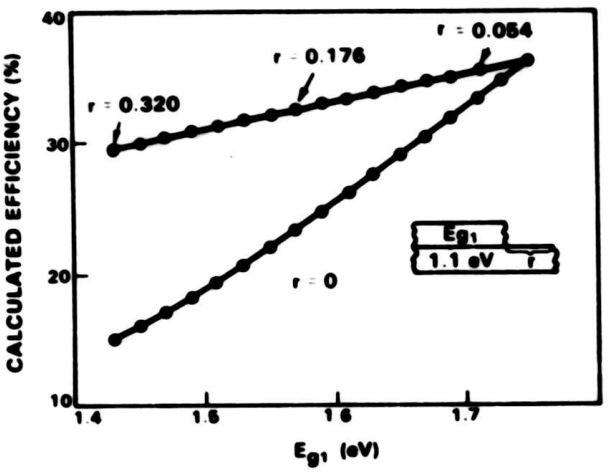

Fig. 18. Plots of calculated AM1 conversion efficiencies of a two-cell, two-terminal tandem cell as a function of the top-cell bandgap energy. The bottom-cell bandgap energy is 1.1 eV. By removing optimal top-cell areas, the conversion efficiencies would be greatly increased.

increase in theoretical combined efficiency at AM1 and 27°C that can be achieved by removing a fraction r of the area of the top cell. The lower curve gives the efficiency as a function of E_{g1} for r = 0, while the upper curve gives the efficiency obtained for the optimal value of r, the value for which the photocurrents of the two cells are equal. The difference is greatest at the lowest values of E_{g1}, where the optimal value of r is greatest. The two curves meet at E_{g1} = 1.75 eV, the optimum value of E_{g1} given by the calculations discussed above, since all those calculations assume r = 0.

Another novel technique that we have developed should be applicable to four-terminal tandem structures as well as two-terminal structures. This is the technique of fabricating ultrathin solar cells by the CLEFT (cleavage of lateral epitaxial films for transfer) process (16-18).

The CLEFT process provides a practical means of separating epilayers from their substrates so that the substrates can be reused for further growth. The key element of this process is the use of lateral epitaxial overgrowth performed by CVD. If a mask with appropriately spaced stripe openings is deposited on a (110) GaAs substrate, the epitaxial growth initiated on the GaAs surface exposed through the openings will be followed by lateral growth over the mask, eventually producing a continuous single-crystal GaAs film that can be grown to any desired thickness. The upper surface of the film is then bonded to a secondary substrate of some other material such as glass. If there is poor adhesion between the mask material and the GaAs, the film will be strongly attached to the GaAs substrate only at the stripe openings. Since a weak plane has been created by the mask and because the (110) plane is the principal cleavage plane of GaAs, the film can be cleaved from the GaAs substrate without degradation of either. We have found that carbonized photoresist is a suitable mask material, since it has the necessary poor adhesion to GaAs and is chemically inert under the conditions that we employ for CVD growth.

Figure 19 is a schematic diagram of the cross section of a CLEFT solar cell (19). The structure

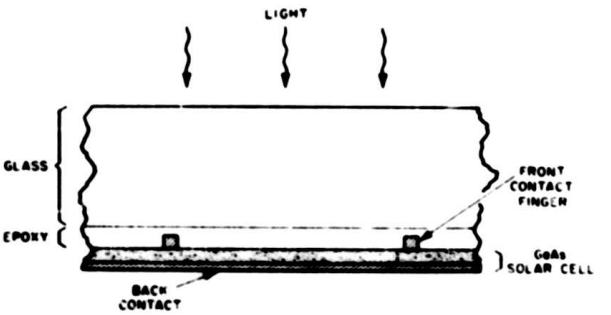

Fig. 19. Cross-sectional view of a completed CLEFT cell, in which the glass substrate serves as the protective cover glass.

of this cell is interesting in several respects. The entire thickness of GaAs is only about 10 μm, compared with 300-400 μm for conventional GaAs solar cells. The glass substrate supports the film and serves as the cover glass for the cell. Another advantageous aspect of the structure is that there are metal contacts on both sides of the GaAs film.

In initial experiments we have made three CLEFT cells, with GaAs films 10 μm thick, that have conversion efficiencies of 15 to 17% at AM1. The 17% cell has an area of 0.51 cm^2 (19). The films for these cells were grown by the $AsCl_3$-GaAs-H_2 method, which is not useful for the growth of GaAs-AlAs or GaAs-GaP alloys. However, we have recently demonstrated lateral overgrowth of GaAs by organometallic chemical vapor deposition (OMCVD), which is suitable for growing these alloys, and we have prepared CLEFT films of GaAs by OMCVD (20).

The CLEFT process is ideal for the fabrication of structures in which films of different semiconductors are stacked on top of one another (17). Instead of the continuous metal contact layer shown at the bottom of the CLEFT cell in Fig. 19, an open contact grid would be used. For optimal operation, this grid should be aligned with the top metal grid of the CLEFT cell, as well as with the top metal grid of the bottom cell. Such a CLEFT cell could be bonded either separately or in

calculated that if 32% of the area of the GaAs cell is removed, the photocurrents generated in the GaAs and Si cells will be equal, and the theoretical combined efficiency will be increased to nearly 30% at AM1.

For two-terminal monolithic tandem structures composed of a bottom Si cell (E_g = 1.1 eV) and top cell with energy gap E_{g1}, Fig. 18 shows the

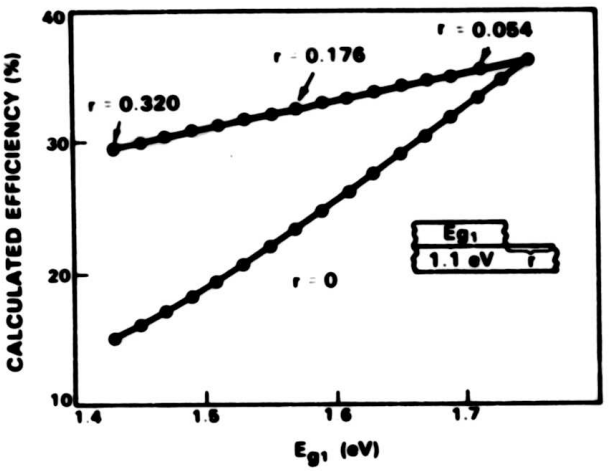

Fig. 18. Plots of calculated AM1 conversion efficiencies of a two-cell, two-terminal tandem cell as a function of the top-cell bandgap energy. The bottom-cell bandgap energy is 1.1 eV. By removing optimal top-cell areas, the conversion efficiencies would be greatly increased.

increase in theoretical combined efficiency at AM1 and 27°C that can be achieved by removing a fraction r of the area of the top cell. The lower curve gives the efficiency as a function of E_{g1} for r = 0, while the upper curve gives the efficiency obtained for the optimal value of r, the value for which the photocurrents of the two cells are equal. The difference is greatest at the lowest values of E_{g1}, where the optimal value of r is greatest. The two curves meet at E_{g1} = 1.75 eV, the optimum value of E_{g1} given by the calculations discussed above, since all those calculations assume r = 0.

Another novel technique that we have developed should be applicable to four-terminal tandem structures as well as two-terminal structures. This is the technique of fabricating ultrathin solar cells by the CLEFT (cleavage of lateral epitaxial films for transfer) process (16-18).

The CLEFT process provides a practical means of separating epilayers from their substrates so that the substrates can be reused for further growth. The key element of this process is the use of lateral epitaxial overgrowth performed by CVD. If a mask with appropriately spaced stripe openings is deposited on a (110) GaAs substrate, the epitaxial growth initiated on the GaAs surface exposed through the openings will be followed by lateral growth over the mask, eventually producing a continuous single-crystal GaAs film that can be grown to any desired thickness. The upper surface of the film is then bonded to a secondary substrate of some other material such as glass. If there is poor adhesion between the mask material and the GaAs, the film will be strongly attached to the GaAs substrate only at the stripe openings. Since a weak plane has been created by the mask and because the (110) plane is the principal cleavage plane of GaAs, the film can be cleaved from the GaAs substrate without degradation of either. We have found that carbonized photoresist is a suitable mask material, since it has the necessary poor adhesion to GaAs and is chemically inert under the conditions that we employ for CVD growth.

Figure 19 is a schematic diagram of the cross section of a CLEFT solar cell (19). The structure

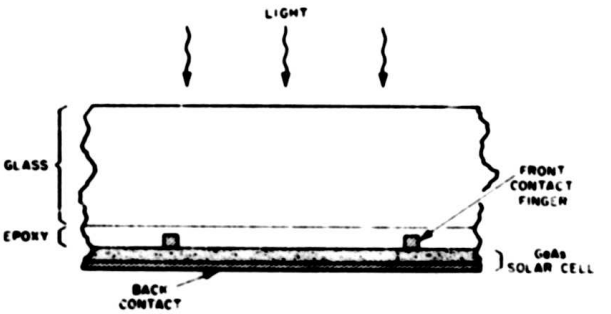

Fig. 19. Cross-sectional view of a completed CLEFT cell, in which the glass substrate serves as the protective cover glass.

of this cell is interesting in several respects. The entire thickness of GaAs is only about 10 μm, compared with 300-400 μm for conventional GaAs solar cells. The glass substrate supports the film and serves as the cover glass for the cell. Another advantageous aspect of the structure is that there are metal contacts on both sides of the GaAs film.

In initial experiments we have made three CLEFT cells, with GaAs films 10 μm thick, that have conversion efficiencies of 15 to 17% at AM1. The 17% cell has an area of 0.51 cm^2 (19). The films for these cells were grown by the $AsCl_3$-GaAs-H_2 method, which is not useful for the growth of GaAs-AlAs or GaAs-GaP alloys. However, we have recently demonstrated lateral overgrowth of GaAs by organometallic chemical vapor deposition (OMCVD), which is suitable for growing these alloys, and we have prepared CLEFT films of GaAs by OMCVD (20).

The CLEFT process is ideal for the fabrication of structures in which films of different semiconductors are stacked on top of one another (17). Instead of the continuous metal contact layer shown at the bottom of the CLEFT cell in Fig. 19, an open contact grid would be used. For optimal operation, this grid should be aligned with the top metal grid of the CLEFT cell, as well as with the top metal grid of the bottom cell. Such a CLEFT cell could be bonded either separately or in

series with a bottom cell, such as a Si cell. If GaAlAs CLEFT cells can be fabricated, a tandem structure formed by bonding such a cell to a Si cell would have a combined maximum theoretical efficiency at AM1 of about 36%, and a practical efficiency of about 30% can be expected. A two-terminal tandem structure is possible if a transparent conductive bonding material is used, while a four-terminal structure is obtained if the bonding material is insulating.

By using the mechanical bonding technique, the lattice matching and connecting junction requirements are eliminated for both two- and four-terminal structures. In a two-terminal structure, if the bandgaps of the two cells are not optimal, opening areas in the top CLEFT cell or bonding this cell to a bottom cell of larger active area can increase the conversion efficiency by raising the photocurrent of the bottom cell. No benefit will result by opening the top cell in the case of four-terminal structures.

ANTIREFLECTION COATINGS

To fabricate the most efficient tandem structures, it is necessary not only to prepare high-quality semiconductor layers and junctions but also to use optimal antireflection (AR) coatings. We will not consider the design of AR coatings in detail. It should be noted, however, that the design will be simpler for two-terminal structures than for four-terminal ones. In the two-terminal case, only the front surface of the top cell requires an AR coating. A multilayer coating will be needed to allow a broad spectrum of solar radiation to be transmitted into the active regions. For a two-cell structure, a double-layer (or at most, a triple-layer) AR coating will be adequate. Since the top cell provides the larger share of the tandem-cell efficiency, the coating design must place a larger emphasis on the top cell. For four-terminal structures, AR coatings are needed on the front and back surfaces of the top cell and on the front surface of the bottom cell. Optical-matching properties must be considered in selecting the bonding layer between the top and bottom cells. Since the top cell makes the larger contribution to the efficiency, the design of the AR coating on the front surface of the top cell is most important.

CONCLUSION

Substantial efficiency increases are expected for two-cell tandem structures in comparison with single-junction cells. Our computer analysis indicates that practical AM1 efficiencies of about 30% at one sun and over 30% at multiple suns can be expected. For AMO, a one-sun efficiency of about 27% is expected. The further increases in efficiency for a three-cell tandem structure are much smaller and may not justify the added complexity. For inexpensive two-cell tandem modules, Si bottom cells are much preferred. For such cells, at AMO and AM1 a top-cell energy gap of 1.75 to 1.80 eV is optimal for both two- and four-terminal structures. The GaAs-AlAs and GaAs-GaP systems are very attractive candidates for the top cell. Significant advances have been achieved in growing GaAs on Ge-coated substrates (for the two-terminal structure), and in obtaining free-standing ultrathin GaAs layers by the CLEFT process (for the two- and four-terminal structures). We believe that these advances will be transferable to the GaAs-AlAs and GaAs-GaP systems. Therefore, high-efficiency, inexpensive two-cell tandem structures for flat-plate and concentrating applications may soon become a reality.

ACKNOWLEDGEMENTS

We acknowledge helpful discussions with J. P. Benner and K. W. Mitchell of the Solar Energy Research Institute, D. J. Flood of the National Aeronautics and Space Administration, and A. J. Strauss, G. W. Turner and R. L. Chapman of Lincoln Laboratory. This work was supported by the Solar Energy Research Institute, the National Aeronautics and Space Administration and the Department of the Air Force.

APPENDIX

Calculations were carried out for one-cell, two-cell and three-cell structures. Here, we will illustrate a two-cell calculation. The other cases are similar. Let the top cell have a bandgap energy E_{g1}, and the bottom cell E_{g2}, with corresponding short-circuit current densities J_{sc1} and J_{sc2}. Since high-quality solar cells have already attained quantum efficiencies values over 90%, we assume 100% quantum efficiency. Then the short-circuit current densities can be written as

$$J_{sc1} = \int_{0.2\ \mu m}^{\lambda_{g1}(\mu m)} q\,F(\lambda)\,d\lambda \qquad (1)$$

$$J_{sc2} = \int_{\lambda_{g1}}^{\lambda_{g2}} q\,F(\lambda)\,d\lambda \qquad (2)$$

where $\lambda_g = 1.239/E_g\ (\mu m)$, q is the electronic charge, and $F(\lambda)$ is the solar photon flux density at λ, which varies with air mass (11).

The open-circuit voltage V_{oc} for each of the cells is given by

$$V_{oc} = \frac{kT}{q} \ln\left(\frac{XJ_{sc}}{J_{oo}} + 1\right) \qquad (3)$$

where X is the concentration ratio, k is Boltzmann's constant, and T is absolute temperature. J_{oo} is the dark saturation current,

and if we assume a simple diffusion current, then

$$J_{oo} = KT^3 \exp\left(-\frac{E_g}{kT}\right) \quad (4)$$

The value of K may be different for different materials. For our calculations of J_{oo} in mA/cm^2, we assume a fixed constant with a value of 0.05. This value was selected so that for AM1 conditions the calculated V_{oc} was 0.97 V for GaAs and 0.66 V for Si, values very close to the respective experimental values of 0.98 (4) and 0.65 V (21).

The fill factor ff for each of the cells is evaluated as follows (22):

$$ff = \frac{V_m}{V_{oc}}\left[1 - \frac{\exp\left(\frac{qV_m}{kT}\right)-1}{\exp\left(\frac{qV_{oc}}{kT}\right)-1}\right] \quad (5)$$

where V_m is given by the relationship

$$\left(\exp\frac{qV_m}{kT}\right)\left(1+\frac{qV_m}{kT}\right) = \frac{XJ_{sc}}{J_{oo}} + 1 \quad (6)$$

For the two-terminal case, the J_{sc} value used in Eqs. 3, 5 and 6 is the same for both cells, namely, the smaller value of J_{sc1} and J_{sc2}. The combined efficiency is then

$$\eta_{tot} = J_{sc}\,(V_{oc})_1(ff)_1 + J_{sc}\,(V_{oc})_2(ff)_2$$

For the four-terminal case, both J_{sc1} and J_{sc2} values are used in Eqs. 3, 5, and 6, and

$$\eta_{tot} = J_{sc1}(V_{oc})_1(ff)_1 + J_{sc2}(V_{oc})_2(ff)_2 \quad (8)$$

With the above equations, η_{tot} can be calculated as a function of E_{g1}, E_{g2}, T, X, and air mass.

To obtain the iso-efficiency curves, values of η_{tot} were first calculated for different combinations of E_{g1} and E_{g2} at fixed T, X and air mass. The curves were then plotted for all combinations of E_{g1} and E_{g2} that produce values of η_{tot} within ± 1% of the η_{tot} values stated on the curves.

REFERENCES

1. D. L. Bowler and M. Wolf, IEEE Trans. Components, Hybrids Manufacturing Technol. CHMT-3, 464 (1980).
2. J. L. Smith, Science 212, 1472 (1981).
3. J. M. Woodall and H. J. Hovel, Appl. Phys. Lett. 30, 492 (1977).
4. J. C. C. Fan, C. O. Bozler and R. L. Chapman, Appl. Phys. Lett. 32, 390 (1978).
5. We have measured efficiencies of about 18% (AM1) for cells, provided by Applied Solar Energy Corp., City of Industry, California.
6. D. Trivich and P. A. Flinn in Solar Energy Research, ed. F. Daniels and J. A. Duffie, (University of Wisconsin Press, Madison, 1955), p. 143.
7. L. M. Fraas and R. C. Knechtli, in Conference Record of the 13th IEEE Photovoltaic Specialists Conference, Washington, DC, 1978 (IEEE, New York, 1978), p. 1196.
8. M. F. Lamorte and D. Abbott, Solid-State Electron. 32, 467 (1979).
9. K. Mitchell, in Conference Record of the 13th IEEE Photovoltaic Specialists Conference, Washington, DC, 1978 (IEEE, New York, 1978) p. 868.
10. S. Sakai and M Umeno, J. Appl. Phys. 51, 5018 (1980).
11. M. P. Thekaekara, Conference of COMPLES, Dahran, Saudi Arabia, November 1975.
12. G. D. Cody, C. R. Wronski, B. Abeles, R. B. Stephens and B. Brooks, Solar Cells 2, 227 (1980).
13. A. A. Bergh and P. J. Dean in Light Emitting Diodes (Clarendon Press, Oxford, 1976), p. 690.
14. R. P. Gale, J. C. C. Fan, B-Y. Tsaur, G. W. Turner and F. M. Davis, IEEE Electron Dev. Lett. EDL-2, 169 (1981).
15. B-Y. Tsaur, J. C. C. Fan, G. W. Turner, F. M. Davis and R. P. Gale, to be published in Conference Record of the 16th IEEE Photovoltaic Specialists Conference, San Diego, September 1982.
16. R. W. McClelland, C. O. Bozler and J. C. C. Fan, Appl. Phys. Lett. 37, 560 (1980).
17. J. C. C. Fan, C. O. Bozler and R. W. McClelland, in Conference Record of the 15th IEEE Photovoltaic Specialists Conference, Kissimmee, Florida, 1981 (IEEE, New York, 1981), p. 666.
18. C. O. Bozler, R. W. McClelland, J. P. Salerno and J. C. C. Fan, J. Vac. Sci. Technol. 20, 720 (1982).
19. C. O. Bozler, R. W. McClelland and J. C. C. Fan, IEEE Electron Dev. Lett. EDL-2, 203 (1981).
20. R. P. Gale, R. W. McClelland, J. C. C. Fan and C. O. Bozler, Appl. Phys. Lett. (to be published).
21. H. T. Weaver, to be published in Conference Record of the 16th IEEE Photovoltaic Specialists Conference, San Diego, September 1982.
22. H. J. Hovel, in Solar Cells, Vol. 2 (Academic Press, New York, 1978), p. 60.

UNCLASSIFIED

SECURITY CLASSIFICATION OF THIS PAGE (When Data Entered)

REPORT DOCUMENTATION PAGE		READ INSTRUCTIONS BEFORE COMPLETING FORM
1. REPORT NUMBER ESD-TR- 83-075	2. GOVT ACCESSION NO. AD-A135 127	3. RECIPIENT'S CATALOG NUMBER
4. TITLE (and Subtitle) Optimal Design of High-Efficiency Tandem Cells		5. TYPE OF REPORT & PERIOD COVERED Journal Article
		6. PERFORMING ORG. REPORT NUMBER MS-6008
7. AUTHOR(s) Fan, John C. Tsaur, Bor-Yeu Palm, Barbara J.		8. CONTRACT OR GRANT NUMBER(s) F19628-80-C-0002
9. PERFORMING ORGANIZATION NAME AND ADDRESS Lincoln Laboratory, M.I.T. P.O. Box 73 Lexington, MA 02173		10. PROGRAM ELEMENT, PROJECT, TASK AREA & WORK UNIT NUMBERS 649L
11. CONTROLLING OFFICE NAME AND ADDRESS Air Force Systems Command, USAF Andrews AFB Washington, DC 20331		12. REPORT DATE September 1982 13. NUMBER OF PAGES 10
14. MONITORING AGENCY NAME & ADDRESS (if different from Controlling Office) Electronic Systems Division Hanscom Air Force Base Bedford, MA 01730		15. SECURITY CLASS. (of this report) UNCLASSIFIED 15a. DECLASSIFICATION DOWNGRADING SCHEDULE n/a

16. DISTRIBUTION STATEMENT (of this Report)

Approved for public release; distribution unlimited.

17. DISTRIBUTION STATEMENT (of the abstract entered in Block 20, if different from Report)

18. SUPPLEMENTARY NOTES

Proc. 16th Photovoltaic Specialists Conf., Sept 82

19. KEY WORDS (Continue on reverse side if necessary and identify by block number)

Solar cell conversion Photovoltaic conversion Tandem cells

20. ABSTRACT (Continue on reverse side if necessary and identify by block number)

Computer analysis indicates that a substantial increase in solar cell conversion efficiencies can be achieved by using two-cell, multi-bandgap tandem structures instead of single-junction cells. Practical AM1 efficiencies of about 30% at one sun and over 30% at multiple suns are to be expected. The further increases in efficiency calculated for a three-cell tandem structure are much smaller and may not justify the added complexity. For inexpensive two-cell tandem modules, Si is preferred for the bottom cell, and the top-cell material should have a bandgap of 1.75 to 1.80 eV. The GaAs-AlAs and GaAs-GaP systems are very attractive candidates for the top cell. Significant advances have been achieved in growing GaAs on Ge-coated Si substrates (for the two-terminal, two-cell structure) and in growing free-standing ultrathin GaAs layers (for the two-terminal or four-terminal structures). These advances should be transferable to the GaAs-AlAs and GaAs-GaP systems.

DD FORM 1 JAN 73 1473 EDITION OF 1 NOV 65 IS OBSOLETE

UNCLASSIFIED

SECURITY CLASSIFICATION OF THIS PAGE (When Data Entered)